Ultrafast Multiharmonic Plasmon Generation by Optically Dressed Electrons

Nicholas Rivera, Liang Jie Wong, Marin Soljačić, and Ido Kaminer

Ultrafast multi-harmonic plasmon generation by optically dressed electrons

Nicholas Rivera[1†], Liang Jie Wong[2], Marin Soljačić[1], and Ido Kaminer[1,3]

[1] *Department of Physics, MIT, Cambridge, MA 02139, USA*
[2] *Singapore Institute of Manufacturing Technology,*
Singapore 138634, Singapore
[3] *Department of Electrical Engineering,*
Technion Israel Institute of Technology, Haifa 32000, Israel.
† *Corresponding author e-mail: nrivera@mit.edu*

Interactions between electrons and photons are a source of rich physics from atomic to astronomical scales. Here, we examine a new kind of electron-photon interaction in which an electron, modulated by light, radiates multiple harmonics of plasmons. The emitted plasmons can be femtosecond in duration and nanometer in spatial scale. The extreme sub-wavelength nature of the plasmons lowers the necessary input light intensity by at least four orders of magnitude relative to state-of-the-art strong-field processes involving bound or free electrons. The results presented here reveal a new means of ultrafast (10-1000 fs) interconversion between photonic and plasmonic energy, and a general scheme for generating spatiotemporally shaped ultrashort pulses in optical materials. More generally, our results suggest a route towards realizing analogues of fascinating physical phenomena like nonlinear Compton scattering in plasmonics and nanophotonics with relatively low intensities, slow electrons, and on nanometer length scales.

Intense optical fields drastically modify the light emission properties of electrons in atomic, molecular and solid-state systems. This modification arises from the fact that the emitting electrons are dressed by the driving field, thus altering their basic physical properties such as energy and momentum [1–9]. At sufficiently large driving fields (the strong-field regime), one can induce radiative processes such as high-harmonic generation (HHG) [10–13] and nonlinear Compton scattering (NLCS) [14–16]. In HHG, a strong driving field causes electrons in atoms and molecules [17–22], or in solids [23–28], to absorb many photons and emit very high harmonics of the driving field. This process is very attractive for producing bright attosecond pulses of high-energy photons in the UV to soft x-ray range. In NLCS, it is not a bound electron but a relativistic free electron, which is interrogated by a strong optical field [14–16]. The result is the conversion of many driving photons into a Doppler-shifted photon and its harmonics (as many as 500 [16]).

Common to HHG and NLCS is the fact that the emission is into the electromagnetic modes of free space. It is both natural and interesting to consider whether these strong-field phenomena could be adapted such that electromagnetic energy is emitted into a general optical medium, e.g. a nanostructured surface, which fundamentally alters the nature of light emission [29–34]. However, achieving strong-field emission phenomena in an optical medium is difficult. This is because processes like HHG and NLCS [35, 36] require very strong fields, which inevitably create complications such as material nonlinearities and material damage.

Here, we propose laser-driven electron modulations near materials supporting nano-confined modes as a means to demonstrate strong-field effects in nanophotonics. In particular, we present a means to generate multiple high harmonics of plasmons from incident light intensities over four orders of magnitude lower than would have been required for an equivalent strong-field effect in free space (such as NLCS). The re-

duced intensities needed are a direct result of the extreme spatial confinement of the plasmons emitted. This allows us to access highly nonlinear free-electron emission in nanophotonic systems at driving fields well below internal atomic fields and below the damage threshold of the relevant materials. In particular, we predict significant generation of multiple high harmonics of graphene plasmons with pump fluences on the order of 1-10 mJ/cm^2 (compared to a damage threshold of around 66-100 mJ/cm^2 [37]). The ability to access strong-field processes in nanophotonics provides a fundamentally new mechanism for coupling between different types of electromagnetic quanta with free electrons (e.g., photons and plasmons).

The scenario we consider is illustrated in Fig. 1(a), where a single electron with initial velocity $\mathbf{v} \equiv c\boldsymbol{\beta}$ travels along the z-direction near a plasmonic film illuminated by a strong laser field of frequency ω_i and wavevector $\mathbf{k}_i$ (c being the speed of light in free space). Due to the translational invariance of the film, the laser alone does not couple to plasmons in the film. The proximity of the electron to the plasmonic film allows the electron to spontaneously emit plasmons of wavevector $\mathbf{q}$ and frequency $\omega_\mathbf{q}$, traveling in the yz-plane at an angle $\theta = \cos^{-1}\left(\frac{\mathbf{q} \cdot \mathbf{v}}{qv}\right)$ relative to the z-direction. Henceforth, unbolded, italicized counterparts of bolded variables denote the magnitude of the respective vectors (e.g. $q = |\mathbf{q}|$). By spontaneous emission (as opposed to stimulated emission), we mean that the plasmon is emitted in the absence of a driving plasmonic field. Here, we consider a normally incident, y-polarized laser pulse (see Figs. 1(a,b)). We show in the Supplementary Information (SI) that our conclusions generalize to other parameter choices.

The mechanism of plasmon emission can be understood both in classical and quantum mechanical terms. In classical terms, the field modulates the electron trajectory and this undulatory motion induces plasmon emission. In quantum terms, the electron stimulatedly absorbs and emits multiple photons of the driving field, causing the electron to sponta-
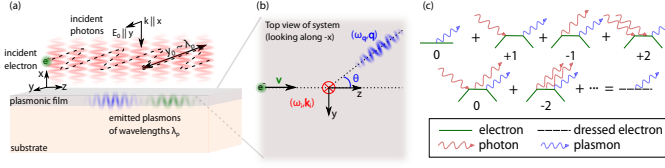
FIG. 1: **Multi-harmonic plasmon generation by optically modulated free electrons.** (a) An intense pulse is incident on an electron moving in the vicinity of a medium supporting highly confined plasmons. The electron converts multiple driving photons into a single plasmon. (b) Top-down view of the scenario in (a). (c) Diagrammatic depiction of ways in which a driving laser can cause plasmon emission by an electron. The many diagrams can equivalently be considered as a first-order transition between laser-driven electron (Floquet) states.

neously emit a plasmon, as illustrated in Fig. 1(c). The frequency of the emitted plasmon, even for fixed angle of emission, depends on the number of quanta of the driving field stimulatedly absorbed or emitted. Thus, for any given angle, there will be plasmons of multiple frequencies ("plasmon harmonics") emitted.

We now determine the intensity of plasmon emission by first considering the laser-driven electron states, which are the Floquet states of the time-periodic Hamiltonian describing the interaction of the electron with the driving laser. That Hamiltonian is $H = \frac{(\mathbf{p}+e\mathbf{A})^2}{2m}$, with e the magnitude of the electron chage and m its mass. This Hamiltonian couples the electron momentum operator $\mathbf{p}$ to the driving vector potential, which in this case is given by $\mathbf{A} = A_0 \cos(\omega_i t)\hat{y}$. The laser-driven electron states are given by

$$
\psi_{\mathbf{k}}(\mathbf{r}, t) = \frac{e^{ik_y y + ik_z z - i\frac{\hbar k^2}{2m}t}}{\sqrt{A}} \times
$$
$$
\exp\left[-\frac{i}{\hbar}\left(\frac{e^2 A_0^2}{4m}t + \frac{eA_0\hbar k_y}{2m\omega_i}\sin(\omega_i t) + \frac{e^2 A_0^2}{8m\omega_i}\sin(2\omega_i t) \right) \right],
$$
(1)

where $\hbar$ is Planck's constant, $\mathbf{k} = (k_y, k_z)$ is the wavevector of the laser-driven electron state, and A is a normalization area. The driving field confers upon the electron an energy spectrum consisting of discrete energies $\frac{\hbar^2 k^2}{2m} + n\hbar\omega_i$, with n being any integer. We now examine the coupling of these laser-driven electron states to the quantized electromagnetic field describing the plasmons.

While the mechanism we propose applies to general nano-optical systems, we assume henceforth for concreteness that the plasmonic film in Fig. 1(a) is graphene. The extreme light confinement possible with graphene plasmons makes it possible to achieve wavelengths over 200 times shorter than the corresponding wavelength of light in free-space [38–47]. For realistic plasmonic losses and wavelengths, the plasmonic field operator is well-described [34] by a quantized scalar potential written as an expansion over evanescent plasmon modes

[38, 40, 47]:

$$
\phi(\mathbf{r}, t) = \sum_{\mathbf{q}} \sqrt{\frac{\hbar\omega_{\mathbf{q}}}{4\epsilon_0 q A}} \left(e^{iq_y y + iq_z z - qx_0 - i\omega_{\mathbf{q}}t} a_{\mathbf{q}} + h.c \right),
$$
(2)

with ϵ_0 being the permittivity of free space, $\mathbf{q} = (q_y, q_z)$ being the plasmonic wavevector, $\omega_{\mathbf{q}}$ being the plasmon frequency set by the dispersion relation of graphene plasmons, and x_0 being the out-of-plane position of the electron. For non-relativistic electrons, the effects of magnetic fields are negligible and x_0 becomes a classical constant of motion. In writing Eq. (2) this way, we have assumed that we operate in a regime where graphene's optical response is linear [68].

We calculate the rate of transitions from an initial state comprising a laser-driven electron state to a final state comprising a different laser-driven electron state and a single plasmon (Fig. 1(c), bottom right). As a result, we obtain a fully analytical expression for the rate of plasmon emission Γ per unit frequency $\omega_{\mathbf{q}}$ and angle of propagation θ, $\frac{d\Gamma}{d\omega_{\mathbf{q}}d\theta}$. It is expressed as a sum over the discrete orders n, each term given by

$$
\frac{d\Gamma_n}{d\omega_{\mathbf{q}}d\theta} = \frac{\alpha\omega_{\mathbf{q}}e^{-2qx_0}}{\beta_{g,\mathbf{q}}} J_n^2(\xi)\text{sinc}^2[(\omega_{\mathbf{q}} - qv\cos\theta - n\omega_i)T],
$$
(3)

with α the fine-structure constant, $\beta_{g,\mathbf{q}}$ the group velocity of the graphene plasmon mode, v the magnitude of the electron velocity, T the interaction time, J_n being the Bessel function of the first kind of order n, and $\xi \equiv \frac{qeE_0}{m\omega_i^2}\sin\theta$, with $E_0 = \omega_i A_0$ being the amplitude of the driving electric field. These expressions are derived in detail in the SI both in a quantum manner and in a classical manner. These two distinct methods of calculation agree when the energy and momentum imparted to the electron by its interaction with photons and plasmons is weak, as is the case for the examples considered in this work.

In Fig. 2, we show the rate of plasmon emission per unit frequency and angle of propagation. In doing so, we have assumed that the graphene is described by a 2D Drude model. In such a model, the dispersion relation is $q = n(\omega)\frac{\omega}{c}$ with $n(\omega) = \frac{\epsilon_r + 1}{4\alpha}\frac{\hbar\omega}{E_f}$, where $n(\omega)$ is the effective index of refraction (or confinement factor), ϵ_r is the substrate permittivity, α is the fine-structure constant, and E_f is the magnitude of the Fermi energy of graphene [38, 40, 41]. Our conclusions are general and do not depend critically on this assumption.

A striking new feature associated with plasmon emission in a strong field is the presence of many discrete spectral peaks at positions given by the zeros of the sinc function in Equation (3): $\omega_{\mathbf{q}} - qv\cos\theta = n\omega_i$. Note that the plasmon harmonic frequencies are generally not evenly spaced due to a combination of strong plasmonic dispersion and Doppler shifts caused by the finite velocity of the electron. Equal spacing is achieved in the case where $v = 0$ or when the plasmon frequency is linear in the plasmon wavevector in the frequency range of interest. In the SI, we show through energy-momentum considerations that n can be interpreted as the number of driving laser pho-
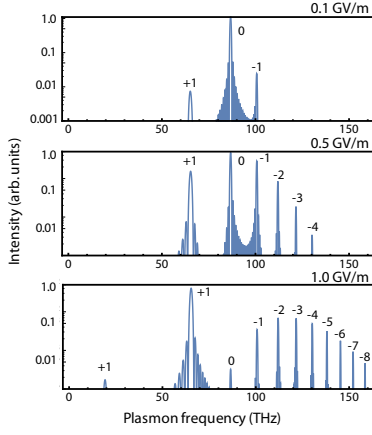
FIG. 2: **Multi-harmonic plasmon generation using relatively weak fields.** Normalized plasmon emission rate for plasmon emission angle $\theta = 1.1$ rad, as a function of driving field and emitted plasmon frequency. For fields of 500 MV/m, we already find that conversion of photons into plasmons is nearly as probable as emission of plasmons with no influence from the driving field.
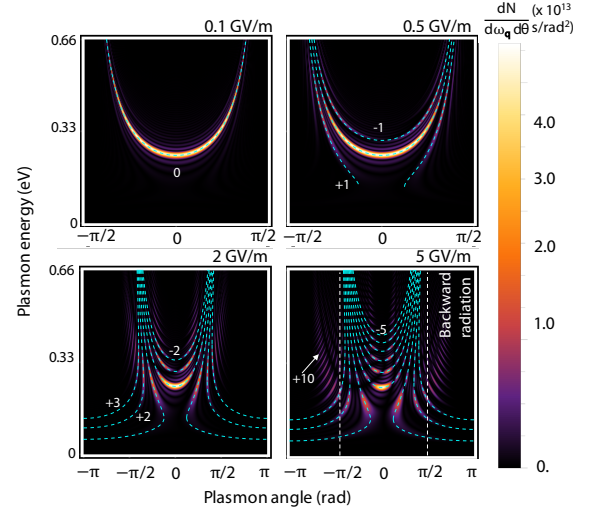

FIG. 3: **Frequency and angle spectrum of multi-harmonic plasmon generation** Colormap of the number of photons emitted per unit plasmon frequency per unit plasmon angle as a function of frequency and angle for a $\beta = 0.02$ electron. The electron 5 nm away from the graphene sheet (doped to -0.5 eV Fermi energy) interacts with a laser field of frequency 16 THz for 250 fs with a field intensities between 100 MV/m and 5 GV/m. The graphene is assumed to be on an optically transparent substrate with an index of refraction of 2. For strong fields, there can be a relatively high probability of plasmon emission accompanied by the absorption or stimulated emission of multiple (as many as 10) driving photons. Overlaid on the colormaps (dashed cyan lines) is the relation between plasmon angle and plasmon frequency prescribed by Equation (3).

tons absorbed by the electron (if n is positive) or stimulatedly emitted (if n is negative). The labels on the peaks in Fig. 2 correspond to this net number of photons absorbed (or stimulatedly emitted) in the emission of a single plasmon. This scheme is also shown in Fig. 1(c) [69].

For weak fields of 100 MV/m (top panel of Fig. 2), the spectrum is dominated by the zero order peak, corresponding to plasmon emission by a free electron in the absence of any driving field (sometimes called plasmonic Cherenkov radiation [48, 49]). At 1 GV/m (bottom panel of Fig. 2), the plasmon spectrum becomes quite intricate, with higher-order processes greatly surpassing the zeroth order process, which dominates at weaker fields. The large frequency and wavevector widths ($\Delta\omega_{\mathbf{q}}$ and Δq respectively) of the peaks at 1 GV/m will correspond to fast temporal variations on the order of $\frac{1}{2\Delta\omega_{\mathbf{q}}} \approx 1$ fs and spatial variations on the order of $\frac{1}{2\Delta q} \approx 1$ nm. Due to the extreme spatial confinement of the emitted plasmons, the resulting plasmon wavelengths (e.g., 10 nm for the -8 peak at 160 THz) are comparable to photon wavelengths of extremely high harmonics (50-100) in conventional HHG.

The mechanism of multi-harmonic plasmon generation due to a strong driving laser field that we study here is quite distinct from HHG and plasmon-enhanced HHG of light [20] in that emission is into a plasmon rather than the far-field [70]. The process considered in this work is also distinct from effects in photon-induced near-field electron microscopy (PINEM) [2–6, 9, 50] and the related electron energy-gain spectroscopy [51, 52]. PINEM involves the energy gain and loss of an electron due to multiple absorption and stimulated emission of a driving field, with effects of spontaneous emission seldom considered [53, 54]. These differences are discussed in SI section "Relation to photon-induced near-field electron microscopy".

Eq. (3) allows us to derive a quantitative estimate of the

field amplitudes E_0 at which higher-order (i.e., $|n| \geq 1$, or multiphoton) effects become prominent. It is E_0 such that $\xi \gtrsim 1$. Physically, $\xi \gtrsim 1$ is equivalent to saying that the amplitude of the electron modulation from the driving field is comparable to the wavelength of emitted electromagnetic wave, leading to an impedance matching between the emitter and the emitted plasmon, which is known to enhance typically inefficient emission processes [34, 56–59]. For a graphene plasmon wavelength of 70 nm (as in [60] for example) and an emission angle such that $\sin\theta \approx 1$, $\xi = 1$ corresponds to E_0 on the order of 500 MV/m, entirely in line with the results found in Fig. 2. If the emission were into a free-space photon of the same frequency, the field needed for $\xi = 1$ would be over 50 GV/m (corresponding to an intensity of about 300 TW/cm^2), which is comparable to atomic scale fields. Fig. 2 along with Equation (3) represent the main result of this work.

In Fig. 3, we expand on Fig. 2 by presenting the full plasmon frequency and plasmon angle dependence of the plasmon emission spectrum of Equation (3). Overlaid on the colormap are lines corresponding to the solutions of the equation $\omega_q - qv\cos\theta = n\omega_i$. The full phase-space dependence of the spectrum reveals two major features. The first is that unlike the order zero process, which can happen in the absence of a driving field, higher-order processes have zero probability to occur when the plasmon is emitted along the direc-

tion of the electron velocity. This is reflected by the factor $J_n^2(\frac{qeE_0}{m\omega_i^2}\sin\theta)$, which is zero when $n \neq 0$ and $\theta = 0$. The second feature is that unlike the plasmon emission that occurs in the absence of a strong field (namely, plasmonic Cherenkov radiation), here plasmons can be emitted in directions opposite the initial electron velocity (i.e., $\frac{\pi}{2} < |\theta| < \pi$). We denote these regions as "backward radiation" (or emission) in Fig. 3. This is noteworthy, as all known schemes for backwards emission in a medium require modes with effective negative indices arising from metamaterials [61–64]. Here, all modes have a positive index but the electromagnetic wave can propagate backwards.

In Fig. 4, we elaborate on the timescale of plasmon emission into different integer bands by plotting the plasmon emission rate Γ into each band ($0, \pm 1, \pm 2, \pm 3, \pm 4, \pm 5$) as a function of the driving field. For weak driving fields, the emission rate into the $|n|$ order follows a power law $E_0^{2|n|} \sim I^{|n|}$, with I being the driving intensity. As a result of this, the different orders are separated in rates by many orders of magnitude for weak fields. For example, for a field of 100 MV/m, the zero order conventional Cerenkov and the fourth order emission process differ by nearly sixteen orders of magnitude. On the other hand, once the field approaches 1 GV/m, even the seemingly unlikely fifth order process (four photons + one plasmon) occurs on nearly picosecond timescales. The field scaling of the lifetimes at these strong fields is no longer a power law; a clear hallmark of a non-perturbative regime. For additional context, we note that the corresponding rate of photon emission into the far field is much lower than the plasmon emission rate in this study. Consider an electron moving at a normalized speed of $\beta = 0.02$ in a 16 THz field of amplitude 5 GV/m. The rate of photon emission (called Thomson scattering in this case) is estimated by the Larmor formula to be 4×10^8 s^{-1}, much less than the value of about 10^{13} s^{-1} for the order ± 1 processes induced by the same drive (see Fig. 4).

In the SI, we generalize the scenario studied here to cases where the electron is relativistic, the light polarization is not restricted to point along the y-axis, and the incident photons propagate in an arbitrary direction. We mention that in this last case, the emitted plasmons satisfy the more general dispersion relation $\omega_q - \mathbf{q} \cdot \mathbf{v} = n(\omega_i - \mathbf{k}_i \cdot \mathbf{v})$.

In summary, we found that non-relativistic electric field strengths (MV/m-GV/m) are sufficient to generate high harmonics of plasmons. Our findings go against the perturbative wisdom that the emission in a medium is always dominated by Cherenkov-like processes which happen in the absence of a driving field, rather than driven processes [35, 65, 66]. These fields can be below the damage threshold in undoped graphene [26, 36, 37]. Further work is needed to determine the exact damage threshold for pulses at lower frequencies and for finite doping in graphene. The concept proposed here applies to general polaritonic (plasmon, phonon, exciton, magnon) materials which have widely different damage thresholds as these materials can be insulators, semiconductors, or metals [67].

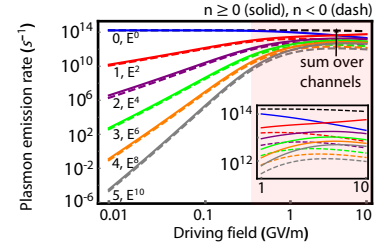From a fundamental perspective, our findings present a

FIG. 4: **Timescales for multi-harmonic plasmon generation:** Rate of plasmon emission associated with 0 through 5 photons being absorbed (+) or stimulatedly emitted (-). $E^{|n|}$ denotes the weak-field power-law scaling of the rates. The black dashed line is the rate summed over channels -5 through 5. The red region denotes where the scaling departs significantly from a power law.

route to take phenomena like NLCS, typically considered in settings of extreme laser facilities, ultrarelativistic electrons, and/or astrophysical settings, and bring them to low intensities, low electron speeds, and nanoscale dimensions. From an applied perspective, these findings may enable new schemes to couple light to plasmons, as well as schemes to achieve increased spatio-temporal resolution in nano-optics, which could be of use for biological and chemical sensing, and imaging at wide range of frequencies.

[1] J. H. Eberly, J. Javanainen, and K. Rzążewski, Physics reports **204**, 331 (1991).
[2] B. Barwick, D. J. Flannigan, and A. H. Zewail, Nature **462**, 902 (2009).
[3] F. J. Garca de Abajo, A. Asenjo-Garcia, and M. Kociak, Nano letters **10**, 1859 (2010).
[4] S. T. Park, M. Lin, and A. H. Zewail, New Journal of Physics **12**, 123028 (2010).
[5] A. Feist, K. E. Echternkamp, J. Schauss, S. V. Yalunin, S. Schäfer, and C. Ropers, Nature **521**, 200 (2015).
[6] L. Piazza, T. Lummen, E. Quinonez, Y. Murooka, B. Reed, B. Barwick, and F. Carbone, Nature communications **6**, 6407 (2015).
[7] C. Kealhofer, W. Schneider, D. Ehberger, A. Ryabov, F. Krausz, and P. Baum, Science **352**, 429 (2016).
[8] S. Beaulieu, A. Comby, A. Clergerie, J. Caillat, D. Descamps, N. Dudovich, B. Fabre, R. Géneaux, F. Légaré, S. Petit, et al., Science **358**, 1288 (2017).
[9] Y. Morimoto and P. Baum, Nature Physics **14**, 252 (2018).
[10] M. Lewenstein, P. Balcou, M. Y. Ivanov, A. L'huillier, and P. B. Corkum, Physical Review A **49**, 2117 (1994).
[11] P. Antoine, A. L'huillier, and M. Lewenstein, Physical Review Letters **77**, 1234 (1996).
[12] I. P. Christov, M. M. Murnane, and H. C. Kapteyn, Physical Review Letters **78**, 1251 (1997).
[13] P. . M. Paul, E. Toma, P. Breger, G. Mullot, F. Augé, P. Balcou, H. Muller, and P. Agostini, Science **292**, 1689 (2001).
[14] E. Esarey, S. K. Ride, and P. Sprangle, Physical Review E **48**, 3003 (1993).
[15] S.-y. Chen, A. Maksimchuk, and D. Umstadter, Nature **396**, 653 (1998).

[16] W. Yan, C. Fruhling, G. Golovin, D. Haden, J. Luo, P. Zhang, B. Zhao, J. Zhang, C. Liu, M. Chen, et al., Nature Photonics **11**, 514 (2017).

[17] Z. Chang, A. Rundquist, H. Wang, M. M. Murnane, and H. C. Kapteyn, Physical Review Letters **79**, 2967 (1997).

[18] P. Salières, B. Carré, L. Le Déroff, F. Grasbon, G. Paulus, H. Walther, R. Kopold, W. Becker, D. Milošević, A. Sanpera, et al., Science **292**, 902 (2001).

[19] B. K. McFarland, J. P. Farrell, P. H. Bucksbaum, and M. Gühr, Science **322**, 1232 (2008).

[20] S. Kim, J. Jin, Y.-J. Kim, I.-Y. Park, Y. Kim, and S.-W. Kim, Nature **453**, 757 (2008).

[21] O. Smirnova, Y. Mairesse, S. Patchkovskii, N. Dudovich, D. Villeneuve, P. Corkum, and M. Y. Ivanov, Nature **460**, 972 (2009).

[22] A. Fleischer, O. Kfir, T. Diskin, P. Sidorenko, and O. Cohen, Nature Photonics **8**, 543 (2014).

[23] A. K. Gupta, O. E. Alon, and N. Moiseyev, Physical Review B **68**, 205101 (2003).

[24] S. Ghimire, A. D. DiChiara, E. Sistrunk, P. Agostini, L. F. Di-Mauro, and D. A. Reis, Nature physics **7**, 138 (2011).

[25] H. Liu, Y. Li, Y. S. You, S. Ghimire, T. F. Heinz, and D. A. Reis, Nature Physics **13**, 262 (2017).

[26] N. Yoshikawa, T. Tamaya, and K. Tanaka, Science **356**, 736 (2017).

[27] M. Sivis, M. Taucer, G. Vampa, K. Johnston, A. Staudte, A. Y. Naumov, D. Villeneuve, C. Ropers, and P. Corkum, Science **357**, 303 (2017).

[28] J. D. Cox, A. Marini, and F. J. G. De Abajo, Nature Communications **8** (2017).

[29] E. M. Purcell, in *Confined Electrons and Photons* (Springer, 1995), pp. 839–839.

[30] D. Kleppner, Physical Review Letters **47**, 233 (1981).

[31] E. Yablonovitch, Physical review letters **58**, 2059 (1987).

[32] L. Novotny and B. Hecht, *Principles of nano-optics* (Cambridge university press, 2012).

[33] M. Pelton, Nature Photonics **9**, 427 (2015).

[34] N. Rivera, I. Kaminer, B. Zhen, J. D. Joannopoulos, and M. Soljačić, Science **353**, 263 (2016).

[35] V. Ginsburg, *Applications of electrodynamics in theoretical physics and astrophysics* (Routledge, 1989).

[36] L. J. Wong, I. Kaminer, O. Ilic, J. D. Joannopoulos, and M. Soljačić, Nature Photonics **10**, 46 (2016).

[37] T. Dong, M. Sparkes, C. Durkan, and W. O'Neill, Journal of Laser Applications **28**, 022202 (2016).

[38] E. Hwang and S. D. Sarma, Physical Review B **75**, 205418 (2007).

[39] Y. Liu, R. Willis, K. Emtsev, and T. Seyller, Physical Review B **78**, 201403 (2008).

[40] M. Jablan, H. Buljan, and M. Soljačić, Physical review B **80**, 245435 (2009).

[41] F. H. Koppens, D. E. Chang, and F. J. García de Abajo, Nano letters **11**, 3370 (2011).

[42] Z. Fei, G. O. Andreev, W. Bao, L. M. Zhang, A. S. McLeod, C. Wang, M. K. Stewart, Z. Zhao, G. Dominguez, M. Thiemens, et al., Nano letters **11**, 4701 (2011).

[43] J. Chen, M. Badioli, P. Alonso-González, S. Thongrattanasiri, F. Huth, J. Osmond, M. Spasenović, A. Centeno, A. Pesquera, P. Godignon, et al., Nature **487**, 77 (2012).

[44] Z. Fei, A. Rodin, G. Andreev, W. Bao, A. McLeod, M. Wagner, L. Zhang, Z. Zhao, M. Thiemens, G. Dominguez, et al., Nature **487**, 82 (2012).

[45] A. Grigorenko, M. Polini, and K. Novoselov, Nature photonics **6**, 749 (2012).

[46] K. Tielrooij, L. Orona, A. Ferrier, M. Badioli, G. Navickaite, S. Coop, S. Nanot, B. Kalinic, T. Cesca, L. Gaudreau, et al., Nature Physics (2015).

[47] M. Jablan, M. Soljacic, and H. Buljan, Proceedings of the IEEE **101**, 1689 (2013).

[48] I. Kaminer, Y. T. Katan, H. Buljan, Y. Shen, O. Ilic, J. J. López, L. J. Wong, J. D. Joannopoulos, and M. Soljačić, Nature communications **7**, ncomms11880 (2016).

[49] F. J. Garcıa de Abajo, ACS nano **7**, 11409 (2013).

[50] G. Vanacore, I. Madan, G. Berruto, K. Wang, E. Pomarico, R. Lamb, D. McGrouther, I. Kaminer, B. Barwick, F. J. G. de Abajo, et al., Nature communications **9**, 2694 (2018).

[51] F. G. de Abajo and M. Kociak, New Journal of Physics **10**, 073035 (2008).

[52] A. Asenjo-Garcia and F. G. de Abajo, New Journal of Physics **15**, 103021 (2013).

[53] Y. Pan and A. Gover, arXiv preprint arXiv:1805.08210 (2018).

[54] A. Gover and Y. Pan, Physics Letters A **382**, 1550 (2018).

[55] P. B. Corkum, Physical Review Letters **71**, 1994 (1993).

[56] N. Rivera, G. Rosolen, J. D. Joannopoulos, I. Kaminer, and M. Soljačić, Proceedings of the National Academy of Sciences p. 201713538 (2017).

[57] Y. Kurman, N. Rivera, T. Christensen, S. Tsesses, M. Orenstein, M. Soljačić, J. D. Joannopoulos, and I. Kaminer, Nature Photonics p. 1 (2018).

[58] F. Machado, N. Rivera, H. Buljan, M. Soljacic, and I. Kaminer, ACS Photonics **5**, 3064 (2018).

[59] P. Schmidt, F. Vialla, S. Latini, M. Massicotte, K.-J. Tielrooij, S. Mastel, G. Navickaite, M. Danovich, D. A. Ruiz-Tijerina, C. Yelgel, et al., Nature nanotechnology p. 1 (2018).

[60] A. Woessner, M. B. Lundeberg, Y. Gao, A. Principi, P. Alonso-González, M. Carrega, K. Watanabe, T. Taniguchi, G. Vignale, M. Polini, et al., Nature materials (2014).

[61] V. G. Veselago, Soviet physics uspekhi **10**, 509 (1968).

[62] R. A. Shelby, D. R. Smith, and S. Schultz, science **292**, 77 (2001).

[63] V. M. Shalaev, Nature photonics **1**, 41 (2007).

[64] Z. Duan, X. Tang, Z. Wang, Y. Zhang, X. Chen, M. Chen, and Y. Gong, Nature Communications **8**, 14901 (2017).

[65] V. Mysakhanyan and A. Nikishov, Zh. Eksp. Teor. Fiz **66**, 1258 (1974).

[66] I. V. Iorsh, A. N. Poddubny, P. Ginzburg, P. A. Belov, and Y. S. Kivshar, Physical review letters **114**, 185501 (2015).

[67] M. Thompson, H. Badakov, A. Cook, J. Rosenzweig, R. Tikhoplav, G. Travish, I. Blumenfeld, M. Hogan, R. Ischebeck, N. Kirby, et al., Physical review letters **100**, 214801 (2008).

[68] Which is accurate if the field driving the electron is isolated from the graphene, or if the optical response of the graphene is negligibly modified by the strong field.

[69] In the language of strong-field processes such as NLCS, the ± 1 orders are understood as Compton scattering of a photon into a plasmon, while $|n| > 1$ orders are understood as NLCS of photons into a plasmon.

[70] As an interesting point of discussion, we note that mechanisms of solid-state HHG in the graphene itself (e.g., theory [23, 28] and experiments [26]), are weaker for the fields considered in Fig. 2.